Nano World Journal

https://doi.org/10.17756/nwj.2023-s2-070

Research Article

Open Access

Optimization of the Adsorption Process of Methylene Blue Dye by Apatites Using a Factorial Design

Ali Boukra[1*], Omar Boukra[1], Souhayla Latifi[1,2], Sanaâ Saoiabi[1], Larbi El Hammari[1] and Ahmed Saoiabi[1]

[1]Laboratoire de Laboratory of Applied Chemistry of Materials, Department of Chemistry, Faculty of Sciences, Mohammed V University, Rabat, Morocco

[2]Laboratory REMTEX, ESITH (Higher school of textile and clothing industries), Casablanca, Morocco

[*]Correspondence to:
Ali Boukra
Laboratoire de Laboratory of Applied Chemistry of Materials,
Department of Chemistry, Faculty of Sciences,
Mohammed V University, Rabat, Morocco.
E-mail: ali.boukra@um5r.ac.ma

Received: July 25, 2023
Accepted: September 26, 2023
Published: September 29, 2023

Citation: Boukra A, Boukra O, Latifi S, Saoiabi S, El Hammari L, et al. 2023. Optimization of the Adsorption Process of Methylene Blue Dye by Apatites Using a Factorial Design. *NanoWorld J* 9(S2): S413-S418.

Published by United Scientific Group

Abstract

In recent years, a number of scientific studies have focused on the preparation and use of grafted HAp. In this context, we have prepared HAp grafted with AMP molecules at different grafting rates in order to precisely improve certain physico-chemical properties to increase the adsorbed amount of methylene blue dye. These materials were synthesized by wet process according to the precipitation method which is carried out by the neutralization of various reagents of calcium ions $Ca(OH)_2$ and phosphate $NH_4H_2PO_4$ at 25 °C in an aqueous medium. The prepared materials HAp and HAp-AMP were characterized by XRD, FTIR, and BET to determine their physicochemical properties. Adsorption of MB dye by apatite matrices was monitored by a factorial design method using Design-Expert software to study the influence of variation and efficiency of different MB concentrations, pH and stirring time between adsorbent and adsorbate to determine optimal conditions for maximum adsorbate retention. The highest removal of MB (328.78 $mg.g^{-1}$) was obtained for an initial concentration of 460 $mg.L^{-1}$, and a contact period of 135.5 min at 298 K.

Keywords

Pollution, Hydroxyapatite, Aminotrimethylene phosphonic acid, Methylene blue, Adsorption, Optimization

Abbreviations

HAp: Hydroxyapatite; AMP: Aminotrimethylene phosphonic acid; HAp-AMP: Hydroxyapatite grafted by aminotrimethylene phosphonic acid; MB: Methylene blue; pH: Potential of hydrogen; XRD: X-ray diffraction; FTIR: Fourier-transform infrared spectroscopy; BET: Brunauer, Emett and Teller; UV-Vis: Ultraviolet-Visible spectroscopy; q_{max}: Adsorption capacity; ANOVA: Analysis of variance; df: Degrees of freedom; Std Dev: Standard deviation; Root MSE: Root-mean-square error; CV: Coefficient of variation.

Introduction

Because of the improper release of industrial effluents into the environment in recent years, water body contamination has become one of the biggest issues on a global scale [1], containing chemical pollutants, specifically minerals and organic compounds [2]. Specifically, pesticides, heavy metals, organic solvents, pharmaceuticals, and dyes [3, 4]. It takes a variety of environmental abilities to intervene in the process of waste of industrial, pharmaceutical, or agricultural origin existing in ecosystems [5].

We shall only discuss dyes in this paper, specifically MB. This is due to the fact that MB, due to its use in industry, is one of the non-biodegradable pollut-

ants that is discharged into the environment the most, specifically into water resources [6]. During printing and dyeing, the textile industry rejects a significant amount of dyes. As a result of the rising demand for efficient and affordable treatment, creative and inexpensive alternatives to adsorbents have been created [7].

The creation of efficient methods for decontaminating polluted locations, which are frequently found in natural or waste waterways, has become crucial in recent years [8]. Examples include chemical precipitation, liquid-liquid extraction, ion exchange, and adsorption onto artificial or natural supports [9, 10]. The latter has a number of benefits, including the ability to economically utilize porous substrates, the recovery of dyes with high added value, and compatibility with policies aimed at environmental preservation [11].

The substance that will serve as the adsorbent in the current investigation is HAp, which has the chemical formula $Ca_{10}(PO_4)_6(OH)_2$. HAp has several uses in the sectors of industry, environmental sanitation, and medicine. It is one of the most novel and promising materials in the biomedical area, as well as a bone or dental substitute, due to its chemical makeup and crystalline structure [12]. Additionally, it is employed in the creation of medication delivery systems for specialized medical care [13, 14]. The preparation of HAp can be done in a number of ways. The best technique should be picked based on the apatite's constituent ions and how they will be used [15]. Wet and dry adsorption are typically the two primary techniques used [16]. The porosity of the supports employed, and the surface chemistry of the produced materials are just two factors that affect adsorption efficiency [5]. In fact, many organic or inorganic chemicals have chemically altered the hydroxyapatite surface [17] to make a more effective composite material and boost the surface's reactivity in order to attain a high adsorption capacity for the elimination of contaminating substances.

In this context, we grafted the $N(\text{-}CH_2\text{-}PO(OH)_2)_3$ (AMP) in variable proportions onto the apatitic matrix $Ca_{10}(PO_4)_6(OH)_2$ in order to improve the physicochemical properties of our material. In particular adsorption efficiency [18].

Materials and Method

Materials

The synthesis of reference HAp is based on the neutralization route which contains the two reagents $Ca(OH)_2$ and $NH_4H_2PO_4$ in aqueous medium. According to the stoichiometry of the following reaction equation with the atomic ratio Ca/P = 10/6 = 1.67. according to the procedure already reported [19].

$$10\,Ca(OH)_2 + 6\,NH_4H_2PO_4 \rightarrow Ca_{10}(PO_4)_6(OH)_2 + 6\,NH_4OH + 12\,H_2O$$

On the other hand, the synthesis of HAp-AMP is subjected to the same precipitation method that described in the case of the reference apatite HAp. However, during the preparation of solution B, the optimal amount for the different proportions of AMP 2.5%, 5%, and 10% is incorporated to that of $NH_4H_2PO_4$. Furthermore, the pH of the solution is always basic (pH >10) regardless of the grafting ratio of AMP, as shown in figure 1. All used materials are nanoscale materials.

Characterization of HAp and HAp-AMP

The porous materials are characterized by the reactivity of their surface considering the substances adjacent to it. At this point, the obtained products were characterized by different suitable physicochemical techniques [8], namely, XRD which was carried out under ambient conditions of temperature and pressure using a Philips PW131 apparatus equipped with a copper anticathode (λ = 1.5454 Å).

FTIR via a VERTEX 70 apparatus (UATRS-CN-RTS-Rabat) with a resolution of 2 cm^{-1}, knowing that the studied spectral range goes from 400 cm^{-1} to 4000 cm^{-1} and also measurement of the specific surface according to the theory of BET with a Micromeritics ASAP2010 apparatus at 77 K and which uses the process of adsorption in multilayers of nitrogen gas at 77 K [18].

Preparation of the MB solution

The preparation is on the one hand the mother solution of adsorbate by diluting a mass of 100 mg in 1 L of aqueous solution and on the other hand, the daughter solutions that had by successive dilutions of the mother solution in a volume of 100 ml of solutions include 5 $mg.L^{-1}$ to 100 $mg.L^{-1}$. The preparation of standards of different concentrations ranging from 5 to 20 $mg.L^{-1}$ in MB to define their absorption range, the concentrations of the prepared solutions were obtained by spectrophotometry UV-Vis, UV-3100pc according to the Beer-Lambert law $A = \varepsilon \ell C$ [20] With: A: absorbance of the solution; ε: molar absorption coefficient of the substance ($L.mg^{-1}.cm^{-1}$); ℓ: optical path length (cm), and C: concentration of the substance ($mg.L^{-1}$).

Adsorption experiment

The adsorption of MB on crude HAp and HAp-AMP composites may have been controlled by both physisorption and chemisorption processes, taking into account initial dye concentration, pH, and adsorption kinetics. The adsorption process is done by direct contact of a reasonable amount of 0.2 g of our material with 100 ml of the solution of pollutant MB,

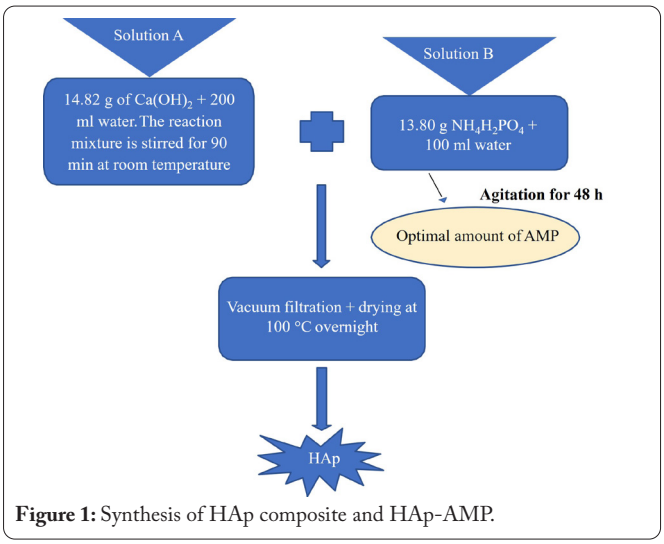

Figure 1: Synthesis of HAp composite and HAp-AMP.

then leaving under agitation at 350 rpm at room temperature which will be analyzed later via UV-Vis spectroscopy to deduce the adsorbed quantities (q_a) by a simple calculation that carries the difference between the initial (C_0) and final (C_e) concentrations according to the following equation [9].

$$q_a = \frac{C_0 - C_e}{m}. V$$

Where q_a: amount of MB adsorbed per unit mass of adsorbent (mg.g^{-1}); C_0: initial concentration of the dye (mg.L^{-1}); C_e: residual concentration of MB at equilibrium (mg.L^{-1}); V: volume of the solution (L); and m: mass of the adsorbent (g).

Study of the parameters

Software developed by some researchers was used to analyze the impacts of various experimental factors (Initial dye concentration studied, pH, and contact time) on the basic adsorptionof MB. All experimental tests were performed according to Design-Expert 11 design matrix. Each factor has three levels, indicated by -1 for lowest, 0 for medium, and +1 for highest (Table 1).The matrix used in this study had 20 runs. All experiments were performed at room temperature. Table 2 shows when the test samples were removed from the shaker.

Table 1: Variable levels for Design-Expert 11 software.

Factors	Symbol	Levels	
		-1	+1
Initial concentration (mg/L)	A	20	500
Contact time (min)	B	2	180
pH	C	3	11

Results and Discussion

XRD analysis

The lines in the XRD diagram were all indexed in the hexagonal system of the $P6_{3/m}$ space group with crystal parameters of a = 9.432 Å and c = 6.882 Å [22]. XRD analysis showed that the grafted apatites were poorly crystallized, however, the crystallite size of HAp by AMP is significantly smaller than that found for HAp [22], confirming the decrease in line intensity with increasing grafting ratio (Figure 2). We also note that all the products prepared have a single apatitic phase, so we can conclude that modification of the HAp surface by AMP leads to no change in the HAp crystalline phase.

FTIR spectroscopy examination

FTIR spectra of the apatites obtained (Figure 3) show the appearance of absorption bands for PO_4^{3-} ions, distinguished by two absorption ranges 1100 - 900 cm^{-1} and 600 - 500 cm^{-1}, which is due to the structural disorder and the nature of the P-O bond, which originates from both inorganic phosphorus (O-P-O) and organic phosphorus (C-P-O). In reality, the assignment of bands linked to PO_3^{2-} phosphonate vibrators in the structure of hybrid apatite are very complicated, due to their overlap with those of PO_4 vibrators. Weak intensities are also observed at 1540, 1480, 1450, 1416, and 875 cm^{-1}, corresponding to the vibrational frequencies of carbonate ions CO_3^{2-} and other carbonyl groups. The absorption bands characterizing OH^- ions in our apatitic material are located at 3560 and 630 cm^{-1}.

Table 2: Plan matrix used in the present study.

Run	Factor 1: A (mg.L^{-1})	Factor 2: B(min)	Factor 3: C	Response: R Quantity adsorbed (mg.g^{-1})
1	15.2	140.368	7.59096	8
2	15.2	140.368	7.59096	8
3	153	9.9	7.6	53
4	153	9.9	7.6	53
5	10	5	12	5
6	185.5	174.05	6.6	58
7	153	140.551	11.84	56
8	153	9.9	7.6	53
9	90.6	250	8.56	57
10	153	140.551	11.84	56
11	270	5	12	62
12	153	140.551	11.84	56
13	90.6	115.25	4	56.5
14	10	5	4	5
15	10	250	12	6.9
16	270	96.875	4	65
17	270	85.85	8.52	65
18	107.5	250	4	50
19	270	250	4	65
20	270	250	9	62

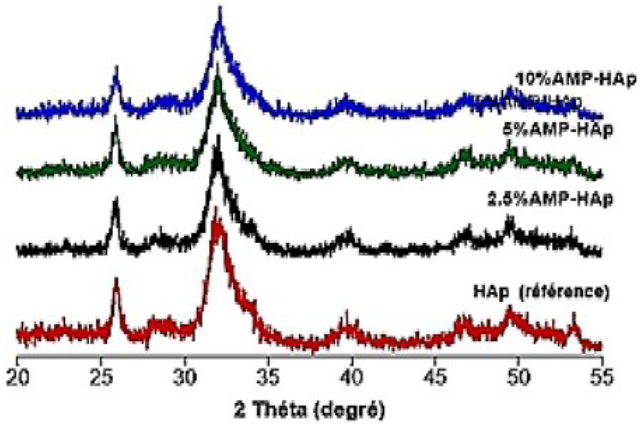

Figure 2: XRD patterns of products HAp-AMP products baked at 100 °C.

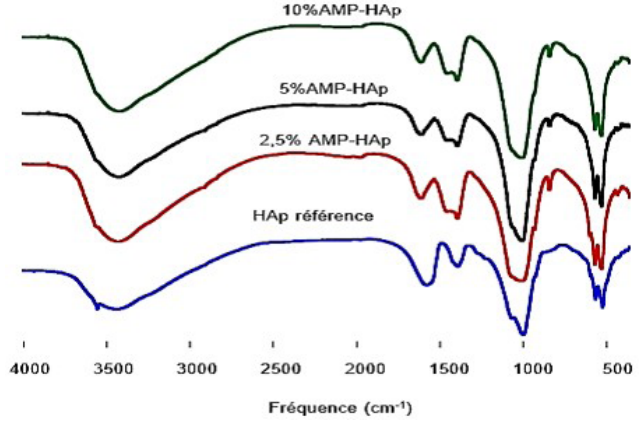

Figure 3: FTIR absorption spectra of HAp-AMP apatites.

BET method

The specific surface area of the synthesized products was determined using nitrogen gas adsorption to measure the pore depth profile. It is clear from the results obtained (Table 3) that the modification of HAp by AMP leads to an increase in specific surface area, and when the specific surface area value of a product is higher, the surface becomes more reactive. This physical property is often one of the key factors in the adsorption process to achieve maximum retention of pollutants [23]. Specific surface areas, volumes, and pore diameters of hybrid apatites compared with reference apatite.

Table 3: Specific surface areas, volumes, and pore diameters of hybrid apatites compared with reference apatite.

	HAp-AMP			
	0%	**2.5%**	**5%**	**10%**
SBET ($m^2.g^{-1}$)	120	159	122	92
Dp (nm)	11	2.2 and 9.5	2.0 and 10.3	1.8 and 9.5

Optimization of the adsorption process

Final equation in terms of coded factors

We can establish the respective effects of the parameters by comparing their coefficients. Thecoded mathematical model with 20 factor levels is described as follows:

Quantity Adsorbed = 45.9403 + 0.206685 * A + 2.66004 * B + 11.5183 * C + 0.000875206 * A * B + 0.0318046 * A * C -0.0754479 * B * C – 0.00057646 * A2 – 0.00863727 * B2 – 1.14255 * C2.

ANOVA

Interactive factors affecting MB dye removal were determined by ANOVA, as presented in table 3.

Fixed effects

The number of degrees of freedom for each source is shown in the "df" column. The total degrees of freedom, according to the surface methodology, is equal to the number of model coefficients added sequentially row by row, as shown in table 4.

P-values less than 0.0005 indicate that the model terms are significant [24]. Inthis case, A, C, AB, BC, B^2, and C^2 are significant model terms. Values greater than 0.1000 mean that themodel term is not significant.

Fit statistics

Based on the statistical modeling, the following criteria will be calculated, as shown in table 5:

- **Std Dev** and the square root of the residual mean square (Root MSE).
- **Mean:** Over all mean of all response data.
- **C.V:** CV, representing the ratio of the Std Dev to the mean.
- **R-squared:** A measure of the amount of variation of the mean from the mean explained by the model.
- **Adjusted R-squared:** It is a measure of the amount of variation around the mean explained by the model, adjusted for the number of terms in the model.

Table 5: Modeling statistics.

Std Dev	37.31	R^2	0.9034
Mean	217.40		
C.V. %	17.16		

Optimization

Optimization of the various factors involved in the adsorption process, namely initial dye concentration, pH, and contact time has been presented in figure 4, following the HAp desirability function rule. To achieve a maximum adsorbed dye quantity of 328.78 $mg.g^{-1}$, it is necessary to operate under optimum conditions for the parameters applied, with an initial dye concentration of 460 $mg.L^{-1}$ and a contact time of 135.5 min. This adsorption process is carried out by dissolution-precipitation of the prepared apatites.

Comparison of the apatite with other reported adsorbents

HAp-AMP was compared with other adsorption materials to assess adsorption performance. Table 6 shows the q_{max} and percentage removal (%) of MB dye from various adsorption materials. As the table shows, the adsorption q_{max} of the MB dye by our products were higher than those of the majority of known adsorbents.

Table 4: Results of variance analysis (ANOVA).

Source	Sum of squares	df	Mean square	F-value	p-value	
Model	1.302E+05	9	14468.63	10.39	0.0005	Significant
A-A	26568.47	1	26568.47	19.09	0.0014	
B-B	51670.83	1	51670.83	37.12	0.0001	
C-C	1318.77	1	1318.77	0.9475	0.3533	
AB	2307.45	1	2307.45	1.66	0.2269	
AC	4667.69	1	4667.69	3.35	0.0970	
BC	3537.53	1	3537.53	2.54	0.1420	
A^2	4303.36	1	4303.36	3.09	0.1092	
B^2	18276.76	1	18276.76	13.13	0.0047	
C^2	1300.33	1	1300.33	0.9342	0.3566	

Table 6: Previous studies on the removal of MB dye from water.

Adsorbent	Optimum condition	Percentage removal (%) or adsorption capacity (q_{max})	Ref.
Bentonite clay/activated charcoal composites	pH = 8	230.30 mg.g^{-1}	[25]
	T = 40 °C		
Cashew nutshell	pH = 10	99.97%	[26]
	Adsorbent dose 2.1846 g.L^{-1}		
	Initial dye concentration 50 mg.L^{-1}		
	Contact time 63 min		
Magnesium ferrite	pH = 11	78.1 mg.g^{-1}	[27]
	Adsorbent dose 1.0 g.L^{-1}		
	Contact time 120 min		
Activated carbon	pH = 6.8	165.17 mg.g^{-1}	[28]
	T = 60 °C		
Sawdust M	pH = 10	7.84 mg.g^{-1}	[29]
	Adsorbate concentration = 20 mg.L^{-1}		
	Adsorbent concentration = 2 g.L^{-1}		
Our study (HAp)	Initial dye concentration 460 mg.L^{-1}	328.78 mg.g^{-1}	Present study

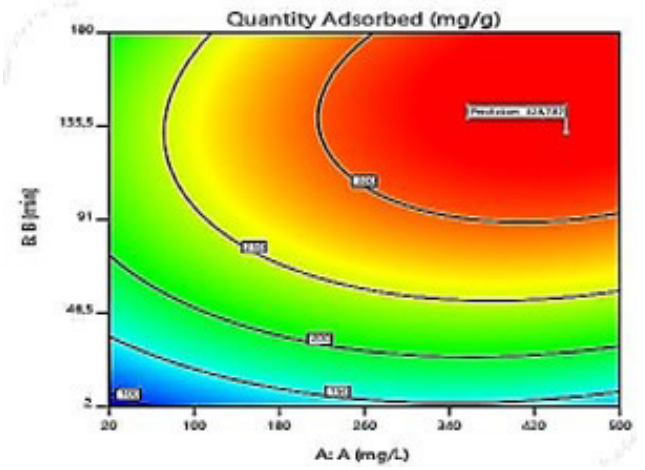

Figure 4: Optimized response.

Conclusion

This study shows how MB dye may be removed from wastewater using nano-HAp and its composites through adsorption. As stated in this article, the composite materials were created by synthesizing an inorganic HAp component while an organic AMP molecule was present. The reference material is pure HAp, which was produced using a stoichiometry of the reaction equation with the atomic ratio Ca/P = 10/6 = 1.67. In line with the precipitation approach. The findings of the characterization using FTIR, XRD, and BET analysis demonstrate that it is possible to modify the apatite surface by grafting AMP to make it more reactive without changing its crystalline structure and thus diminishing the crystallinity of the powder. The main goal of this study is to determine the optimal conditions for maximum MB retention. Design-Expert 11 software was used to achieve this goal. The results show that in order to achieve a maximum amount of adsorption of nearly 328.78 mg.g^{-1}, we must work under the experimental conditions of the various parameters used, namely 460 mg.L^{-1} and a stirring time of 135.5 min, while pH does not have a frequent impact on adsorption. Future study on creating useful uses for these intriguing HAp-based materials is strongly advised. These materials could be used, for example, as effective adsorbents for other non-biodegradable contaminants. And secondly, to create novel delivery systems to enhance the quality of life for patients.

Acknowledgements

The authors would like to thank the Mohammed V University of Rabat, Morocco, for the financial support of this work.

Conflict of Interest

The authors declare that they have no conflict of interest.

References

1. Moussadik A, Lazar NE, Mazkad D, Brigiano FS, Baert K, et al. 2023. Investigation of electronic and photocatalytic properties of $AgTi_2(PO_4)_3$ NASICON-type phosphate: combining experimental data and DFT calculations. *J Photochem Photobiol A Chem* 435: 114289. https://doi.org/10.1016/j.jphotochem.2022.114289
2. Anouzla A, Kastali M, Azoulay K, Bencheikh I, Fattah G, et al. 2022. Multi-response optimization of coagulation-flocculation process for stabilized landfill leachate treatment using a coagulant based on an industrial effluent. *Desalin Water Treat* 254: 71-79. https://doi.org/10.5004/dwt.2022.28388
3. Abdel-Aty AM, El-Dib MA, Badawy MI. 2006. Toxicity of pesticide industrial wastewater to the green alga *Scenedesmus obliquus*: a case study. *Pak J Biol Sci* 9(3): 563-567. https://doi.org/10.3923/pjbs.2006.563.567
4. Bhatia M, Goyal D. 2014. Analyzing remediation potential of wastewater through wetland plants: a review. *Environ Prog Sustain Energy* 33(1): 9-27. https://doi.org/10.1002/ep.11822
5. Bouyarmane H. 2014. Etude des processus d'adsorption et de photodégradation des polluants organiques supportés sur les composites TiO_2-Apatite. Mohammed V Université. (Doctoral dissertation)
6. Weng CH, Pan YF. 2007. Adsorption of a cationic dye (methylene blue) onto spent activated clay. *J Hazard Mater* 144(1-2): 355-362. https://doi.org/10.1016/j.jhazmat.2006.09.097
7. Abrouki Y, Mabrouki J, Anouzla A, Rifi SK, Zahiri Y, et al. 2021. Optimization and modeling of a fixed-bed biosorption of textile dye using

agricultural biomass from the Moroccan Sahara. *Desalin Water Treat* 240: 144-151. https://doi.org/10.5004/dwt.2021.27704

8. Loukilia H, Mabroukic J, Anouzlab A, Kouzia Y, Younssia SA, et al. 2021. Pre-treated Moroccan natural clays: application to the wastewater treatment of textile industry. *Desalin Water Treat* 240: 124-136. https://doi.org/10.5004/dwt.2021.27644
9. Chen Q, Yao Y, Li X, Lu J, Zhou J, et al. 2018. Comparison of heavy metal removals from aqueous solutions by chemical precipitation and characteristics of precipitates. *J Water Process Eng* 26: 289-300. https://doi.org/10.1016/j.jwpe.2018.11.003
10. Mohammed AA, Selman HM. 2018. Liquid surfactant membrane for lead separation from aqueous solution: studies on emulsion stability and extraction efficiency. *J Environ Chem Eng* 6(6): 6923-6930. https://doi.org/10.1016/j.jece.2018.10.021
11. Rafatullah M, Sulaiman O, Hashim R, Ahmad A. 2010. Adsorption of methylene blue on low-cost adsorbents: a review. *J Hazard Mater* 177(1-3): 70-80. https://doi.org/10.1016/j.jhazmat.2009.12.047
12. Monma H, Kitami Y, Tsutsumi M. 1994. Characterization of Electrolytically Prepared Calcium-Deficient Apatite Single Crystals. In Mizutani N, Akashi K, Kimura T, Ohno S, Yoshimura M (eds) Advanced Materials'93. Elsevier, pp 781-784.
13. Ginebra MP, Canal C, Espanol M, Pastorino D, Montufar EB. 2012. Calcium phosphate cements as drug delivery materials. *Adv Drug Deliv Rev* 64(12): 1090-1110. https://doi.org/10.1016/j.addr.2012.01.008
14. Loca D, Locs J, Dubnika A, Zalite V, Berzina-Cimdina L. 2015. Porous Hydroxyapatite for Drug Delivery. In Mucalo M (ed) Hydroxyapatite (HAp) for Biomedical Applications. Woodhead Publishing, pp 189-209.
15. Zahouily M, Abrouki Y, Bahlaouan B, Rayadh A, Sebti S. 2003. Hydroxyapatite: new efficient catalyst for the Michael addition. *Catal Commun* 4(10): 521-524. https://doi.org/10.1016/j.catcom.2003.08.001
16. Narasaraju TSB, Phebe DE. 1996. Some physico-chemical aspects of hydroxylapatite. *J Mater Sci* 31: 1-21. https://doi.org/10.1007/BF00355120
17. Anwar A, Rehman IU, Darr JA. 2016. Low-temperature synthesis and surface modification of high surface area calcium hydroxyapatite nanorods incorporating organofunctionalized surfaces. *J Phys Chem C* 120(51): 29069-29076. https://doi.org/10.1021/acs.jpcc.6b05878
18. Saoiabi S, El Asri S, Laghzizil A, Saoiabi A, Ackerman JL, et al. 2012. Lead and zinc removal from aqueous solutions by aminotriphosphonate-modified converted natural phosphates. *Chem Eng J* 211: 233-239. https://doi.org/10.1016/j.cej.2012.09.017
19. Saoiabi S, Achelhi K, Masse S, Saoiabi A, Laghzizil A, et al. 2013. Organo-apatites for lead removal from aqueous solutions: a comparison between carboxylic acid and aminophosphonate surface modification. *Colloids Surf A Physicochem Eng Aspects* 419: 180-185. https://doi.org/10.1016/j.colsurfa.2012.12.005
20. Kifuani KM, Mayeko AKK, Vesituluta PN, Lopaka BI, Bakambo GE, et al. 2018. Adsorption of a basic dye, methylene blue, in aqueous solution, on a bioadsorbent from agricultural waste of *Cucumeropsis mannii* Naudin. *Int J Biol Chem Sci* 12(1): 558-575. https://doi.org/10.4314/ijbcs.v12i1.43
21. Hammari LEL, Laghzizil A, Barboux P, Lahlil K, Saoiabi A. 2004. Retention of fluoride ions from aqueous solution using porous hydroxyapatite: structure and conduction properties. *J Hazard Mater* 114(1-3): 41-44. https://doi.org/10.1016/j.jhazmat.2004.06.032
22. Farzadi A, Bakhshi F, Solati-Hashjin M, Asadi-Eydivand M, Osman NA. 2014. Magnesium incorporated hydroxyapatite: synthesis and structural properties characterization. *Ceram Int* 40(4): 6021-6029. https://doi.org/10.1016/j.ceramint.2013.11.051
23. da Silva OG, da Silva Filho EC, da Fonseca MG, Arakaki LN, Airoldi C. 2006. Hydroxyapatite organofunctionalized with silylating agents to heavy cation removal. *J Colloid Interface Sci* 302(2): 485-491. https://doi.org/10.1016/j.jcis.2006.07.010
24. Blume JD, Greevy RA, Welty VF, Smith JR, Dupont WD. 2019. An introduction to second-generation p-values. *Am Stat* 73(sup1): 157-167. https://doi.org/10.1080/00031305.2018.1537893
25. Chagas NV, Meira JS, Anaissi FJ, Melquiades FL, Quinaia SP, et al. 2014. Preparation, characterization of bentonite clay/activated charcoal composites and 23 factorial design application in adsorption studies of methylene blue dye. *Rev Virtual Quim* 6(6): 1607-23. https://doi.org/10.5935/1984-6835.20140104
26. Subramaniam R, Ponnusamy SK. 2015. Novel adsorbent from agricultural waste (cashew nut shell) for methylene blue dye removal: optimization by response surface methodology. *Water Resour Ind* 11: 64-70. https://doi.org/10.1016/j.wri.2015.07.002
27. Ivanets A, Prozorovich V, Roshchina M, Sychova O, Srivastava V, et al. 2022. Methylene blue adsorption on magnesium ferrite: optimization study, kinetics and reusability. *Mater Today Commun* 31: 103594. https://doi.org/10.1016/j.mtcomm.2022.103594
28. Rosli NA, Ahmad MA, Noh TU. 2023. Unleashing the potential of pineapple peel-based activated carbon: response surface methodology optimization and regeneration for methylene blue and methyl red dyes adsorption. *Inorg Chem Commun* 155: 111041. https://doi.org/10.1016/j.inoche.2023.111041
29. Bouyahia C, Rahmani M, Bensemlali M, El Hajjaji S, Slaoui M, et al. 2023. Influence of extraction techniques on the adsorption capacity of methylene blue on sawdust: optimization by full factorial design. *Mater Sci Energy Technol* 6: 114-123. https://doi.org/10.1016/j.mset.2022.12.004